

AN INVESTIGATION OF METHODS
OF ATTENUATION MEASUREMENT
IN X-BAND WAVEGUIDE

A Thesis
Presented to
the Faculty of Graduate Studies and Research
The University of Manitoba

In Partial Fulfillment
of the Requirements for the Degree
Master of Science in Electrical Engineering

by
Klaus Wolfgang Floch

October 1965



ACKNOWLEDGEMENT

The author wishes to sincerely thank the National Research Council for its financial assistance and Professor Ernest Bridges of the University of Manitoba for his guidance through this project.

ABSTRACT

The r.f. and i.f. substitution methods of measuring attenuation in X-band waveguides are outlined. The problem of frequency stabilization is presented. A system which locks the local oscillator frequency to the signal generator frequency with a 30 MHz difference is designed and tested. A system which minimizes the effects of frequency drift in the i.f. substitution method is proposed and tests made using this system are discussed.

TABLE OF CONTENTS

| CHAPTER | | PAGE |
|---------|--|------|
| I | INTRODUCTION | 1 |
| II | METHODS OF INSERTION LOSS MEASUREMENTS | 3 |
| | The R.F. Substitution Method | 3 |
| | The I.F. Substitution Method | 5 |
| | Extensions of the I.F. Substitution Method. | 8 |
| III | STABILIZATION SYSTEM REQUIREMENTS | 10 |
| | The Reflex Klystron | 10 |
| | A Frequency Tracking System | 16 |
| IV | INTERMEDIATE FREQUENCY STABILIZATION | 18 |
| | I.F. Amplifier | 18 |
| | The Ratio Detector | 21 |
| | The Stabilizing Loop | 23 |
| | Discussion of Results | 25 |
| V | ATTENUATION MEASUREMENTS | 26 |
| | Measurements with the Open Loop | 26 |
| | An Improved System | 28 |
| VI | INTERPRETATION OF RESULTS | 31 |
| | Test Results | 31 |
| | System Evaluation | 33 |
| | Discussion of Results | 35 |
| | Conclusions | 35 |

Table of Contents (Continued)

| CHAPTER | PAGE |
|---|------|
| APPENDIXES | |
| A DESIGN PROCEDURES | 38 |
| I.F. Amplifier Design | 38 |
| Ratio Detector Design | 41 |
| B REFLEX KLYSTRON CHARACTERISTICS | 45 |
| C TABLES OF RESULTS | 47 |
| BIBLIOGRAPHY | 50 |

LIST OF FIGURES

| FIGURE | PAGE |
|--|------|
| 1 Schematic for the R.F. Substitution Method | 4 |
| 2 Basic System for the I.F. Substitution Method | 6 |
| 3 Gainsborough's Parallel I.F. Substitution Method . | 8 |
| 4 Schematic of a Reflex Klystron | 11 |
| 5 Time-Position Diagram Showing the Bunching Process of a Reflex Klystron | 12 |
| 6 Operating Modes of a Reflex Klystron | 15 |
| 7 Frequency Tracking System | 17 |
| 8 Flat Staggered Pair I.F. Amplifier | 19 |
| 9 Single Tuned Amplifier | 20 |
| 10 Ratio Detector | 22 |
| 11 Ratio Detector Characteristic | 23 |
| 12 Open Loop System for the I.F. Substitution Method. | 27 |
| 13 Improved System for the I.F. Substitution Method . | 29 |
| 14 Measurement Results | 32 |
| A.1 Schematic for Obtaining Klystron Characteristic .. | 45 |
| A.2 2K25 Klystron Characteristic | 46 |

LIST OF TABLES

| TABLE | | PAGE |
|-------|---|------|
| 1 | Results with Screen in Place | 47 |
| 2 | Results without Screen | 48 |
| 3 | Results with Maximum Attenuation Measurable | 49 |

CHAPTER I

INTRODUCTION

A very important facet of microwave measurements is the determination of the attenuation, or insertion loss, of two-port devices. If the attenuation is below 30 db, measurements can be made easily by what is known as the r.f. substitution method^{1*}. However, because of the low power levels involved, attenuations greater than 30 db require a more complex system.

This more complex method is the i.f. substitution method¹. Problems inherent in this method and their solution as applied to X-band waveguide equipment, are discussed in this thesis.

In Chapter II, both the r.f. and i.f. substitution methods are outlined and their relative merits are discussed. It is pointed out that frequency drift is the major problem associated with the i.f. substitution method.

A qualitative analysis of reflex klystron theory is presented in Chapter III. A frequency stabilization system based on the results of the theory of reflex klystrons is proposed.

The individual blocks of the stabilizing loop are discussed in Chapter IV. The results of tests on the system as a whole are

* The numeral denotes reference number as listed in the bibliography.

presented and discussed.

In Chapter V, attempts to measure attenuation without frequency stabilization are discussed. A system to minimize effects of frequency drift is proposed. The results obtained using the proposed system are presented in Chapter VI. The system is evaluated on the basis of these results, and a summarizing discussion of obtained results is given. Conclusions arrived at are given and suggestions for improvement on the stabilizing loop are made.

In Appendix A, i.f. amplifier and ratio detector design calculations are given. Tests to obtain the operating characteristics of the 2K25 klystron are described in Appendix B and the results are given. The results of attenuation measurements are presented in tabular form in Appendix C.

CHAPTER II

METHODS OF INSERTION LOSS MEASUREMENTS

The insertion loss of a device can be defined as "the ratio, in db, of the power received at the load before insertion of the apparatus to the power received at the load after insertion"². This definition immediately leads to the basic procedure for insertion loss, i.e. attenuation measurements. This method and an extension of it will be discussed in this chapter.

Weinschel¹ points out that the above definition leads to a non-unique value of insertion loss, its value depending on transmission line impedance and load impedance. A more restricted definition of insertion loss results, which requires the input and the output of the device to be match terminated, i.e. reflectionless³. This requirement yields a unique insertion loss for a device. In the following discussion, matched conditions will be assumed.

The R.F. Substitution Method

This method of attenuation measurement follows directly from the above definition. The device to be tested is inserted as shown in Figure 1. The attenuator is set to about 10 db to provide isolation of the generator from the load. The power, P_1 , received by a matched r.f. detector, generally a thermistor, is measured with the power meter. The device is then removed and the rest of the system is left

unchanged. Again the power at the matched load, i.e. the detector, is measured. If this value is now P_2 , then the insertion loss or attenuation is given by:

$$A = 10 \log_{10} \frac{P_2}{P_1} \dots\dots\dots 2.1$$

A more sophisticated and more direct procedure, which yields a direct reading of attenuation, thus eliminating calculations, is possible if a calibrated, precision attenuator is available. The device is inserted and the attenuator set to zero db of attenuation. The power at the load, P_1 , is determined. The device is removed and the attenuator setting is increased until the power at the load is again P_1 . The setting of the attenuator plus its insertion loss then gives the attenuation through the test device. The insertion loss of the attenuator may be measured by the procedure discussed above. A typical measurement setup is shown in Figure 1.

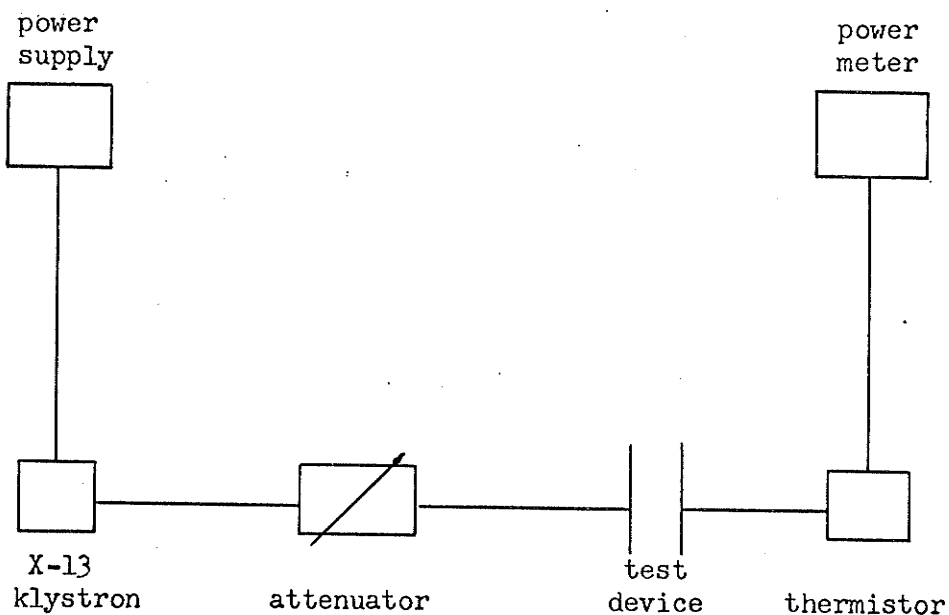


Figure 1: Schematic for the r.f. substitution method.

The great advantage of this method is its simplicity and directness. Reflex klystrons usually have good short term power stability and hence the time lag due to removal of the device under test does not result in any appreciable errors.

However, there exist serious limitations on the range of attenuations measurable. These limitations are determined by the maximum power available from the klystron oscillator and the minimum power level measurable. At low power levels, thermistor drift also causes problems and care must be taken to eliminate drift by continual adjustment of the thermistor bias current.

With the waveguide equipment available, attenuations of the order 40 db are measurable. However, the low power levels involved and the inaccuracy of the variable precision attenuator at such high settings create an error of about ± 1 db.

The I.F. Substitution Method

The i.f. substitution method offers a system with a much greater dynamic range than the r.f. substitution method, without loss of accuracy. The increased range of measurement is made possible by the use of high gain amplifiers, which minimizes the effects of low power levels. Since high gain amplifiers at the frequencies used in this case are hard, if not impossible, to realize, an intermediate frequency signal, proportional in amplitude to the strength of the original signal, must be used.

This requires the measurement setup shown in Figure 2. The mixer gives a 30 MHz output proportional to the signal strength, and is registered as a D.C. current detected by a test receiver. The receiver has a variable gain as well as a 30 MHz attenuator at the i.f. input.

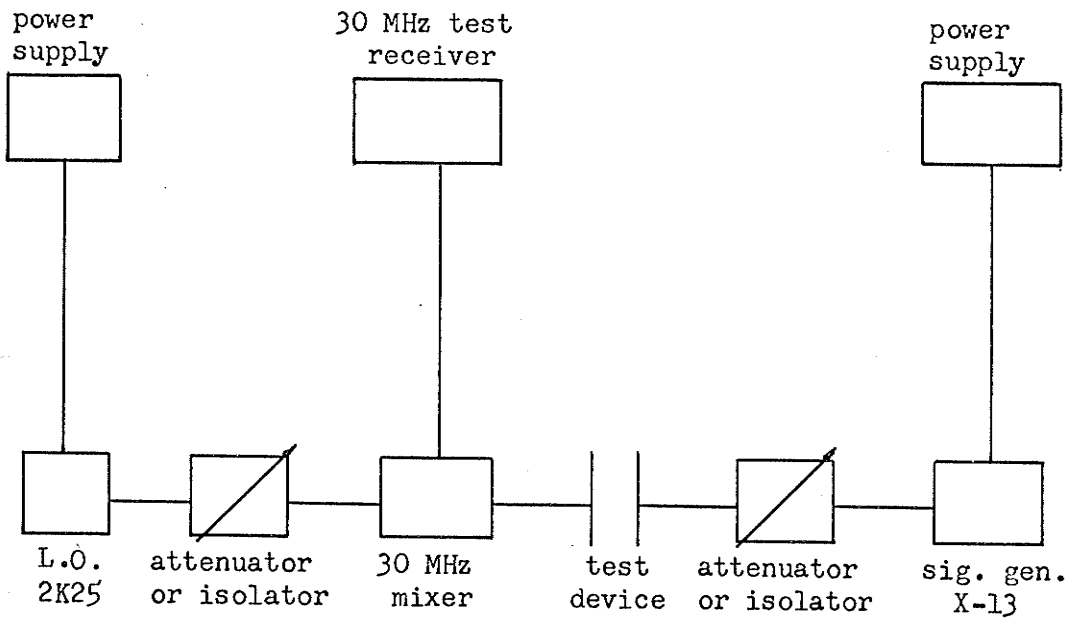


Figure 2: Basic system for the i.f. substitution method

The measurement procedure is quite the same as for the r.f. substitution method. The device is inserted. The gain of the receiver is adjusted to give some convenient reading of current. Then the device is removed and the input attenuation of the receiver is increased until the same current reading is obtained. The difference in attenuator settings gives the insertion loss of the device.

The major disadvantage of the i.f. substitution method is that the signal generator and the local oscillator must have a high degree

of frequency stability. For X-band waveguide, the most common generator is the reflex klystron. As will be shown in the next chapter, reflex klystron frequency is a function of reflector voltage and frequency change is quite high for a small reflector voltage change. Since most 30 MHz i.f. equipment is relatively narrow, i.e. about 3 MHz, a small change in the frequency of the signal generator or local oscillator will change the mixer output frequency appreciably. For instance, a signal at 10 GHz might very easily change by 1 MHz, which represents a 0.01% frequency drift. This 1 MHz change will also appear in the output frequency of the mixer. This puts the i.f. signal almost outside the passband of the i.f. amplifier, causing a change in the detected output. Thus frequency stability of the signal generator and local oscillator has to be better than 0.01%.

Other disadvantages of course exist. A major one is the non-linearity of the mixer and the detector. Linearity, in this case, means that the ratio of output amplitude to input amplitude remains constant with varying input amplitude. The linearity ranges of the mixer and the detector usually dictate the smallest attenuation measurable in one step, thus limiting the range of measurements possible. At low power levels, system noise also starts to have effects and creates an upper limit on the measurement range. These limits of course depend on the accuracy required, becoming more restricted as accuracy is increased.

Extensions of the I.F. Substitution Method

With care and more complex systems than that shown in Figure 2, the dynamic range of the i.f. substitution method can be increased without loss of accuracy. Gainsborough⁴ developed the "parallel i.f. substitution method" with which detector and mixer linearity limitations and errors due to noise were reduced to a minimum. He was able to measure signal levels about 16 db below noise to an accuracy of $\pm 1/2$ db. He claimed that with signal strengths comparable to the noise level, accuracy was unimpaired.

Gainsborough's system as applied to attenuation measurements would take the form shown in Figure 3. A measurement would proceed as follows. With the device removed, the standard attenuator is set

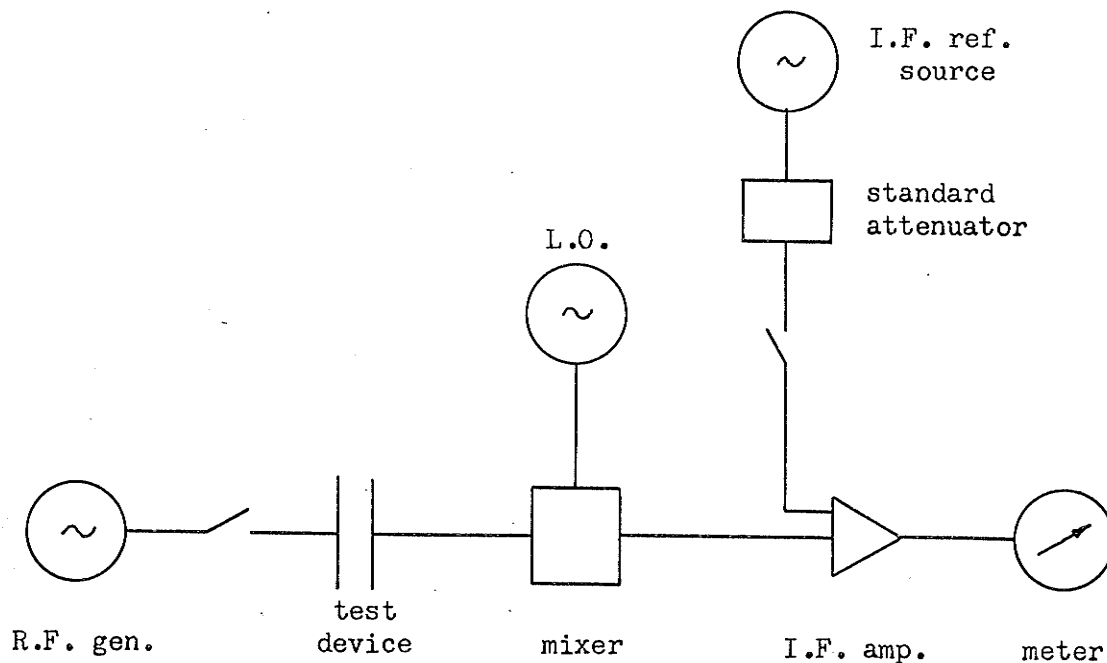


Figure 3: Gainsborough's parallel i.f. substitution method

to give a meter deflection equal to the deflection caused by the mixer output. The device is inserted and again the standard attenuator is set to give equal meter deflections from either arm. The difference in attenuator settings then gives the attenuation of the device.

The accuracy of Gainsborough's method is further increased over the basic i.f. substitution method by the use of i.f. attenuators. Since i.f. attenuators are only used at the intermediate frequency, for example 30 MHz, they can be calibrated much more accurately than r.f. attenuators, which are usually constructed to cover a wide frequency band. Furthermore, matching of the attenuator impedance to the system impedance is easier and can be accomplished to a higher degree of accuracy than for r.f. attenuators because, again, the i.f. attenuator is meant for only a very narrow bandwidth.

Weinschel¹ improved Gainsborough's system by introducing an automatic gain control, AGC, circuit to regulate i.f. amplifier gain and an automatic frequency following, AFF, circuit to change the local oscillator frequency to track frequency changes of the r.f. source. Furthermore, the switching between the paths is done automatically by a 1000 Hz signal. Weinschel was able to measure attenuations from -15 dbm to -121 dbm. Mixer non-linearity caused a 0.1 db deviation at -15 dbm, while fluctuations due to noise in the output caused 0.2 db error at -121 dbm.

CHAPTER III

STABILIZATION SYSTEM REQUIREMENTS

To determine the requirements and the nature of the tracking system, the operating characteristics of the reflex klystron must be known. These are discussed in this chapter and the required system is developed in block diagram form.

The Reflex Klystron

A completely rigorous theoretical development of the operation of a reflex klystron is very complex and excellent texts on the subject have been published^{5,6}. However, a qualitative analysis, such as given by Ginzton⁷, will suffice for the purposes of this discussion.

The fundamental concept that a decelerating charged particle yields energy to an electromagnetic field is utilized in klystrons. A schematic of reflex klystron construction is shown in Figure 4. Electrons are emitted by the cathode and are accelerated towards the cavity. An r.f. field exists in the cavity, oscillating at the resonant frequency of the cavity. Depending on their time of entry, electrons are either accelerated or decelerated by the sinusoidally varying r.f. field. On leaving the cavity, the electrons have different velocities and the beam is said to be velocity modulated. If the electrons are now allowed to drift under the effect of a time

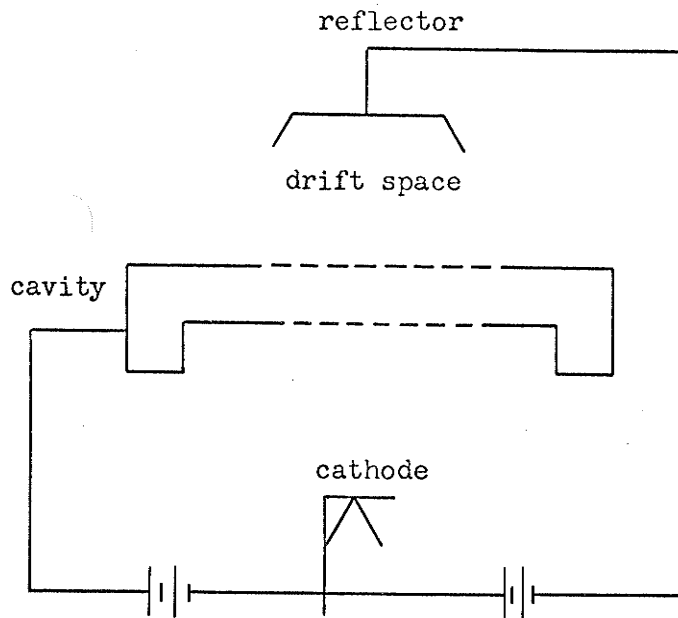


Figure 4: Schematic of a reflex klystron

invariant field, they will form into bunches, i.e. a density modulated beam of electrons. Density modulation takes place in the drift space, where the beam is also turned around by the negative potential on the reflector. Upon reentering the cavity, the beam is in the form of electron bunches and deceleration of a bunch will cause the energy of the field in the cavity to increase. If the increase is greater than the energy required to sustain oscillations and to overcome losses, the excess energy can be coupled out of the cavity by a loop antenna or through an iris. A means of graphically showing the bunching process is given by Ginzton⁷ and shown in Figure 5.

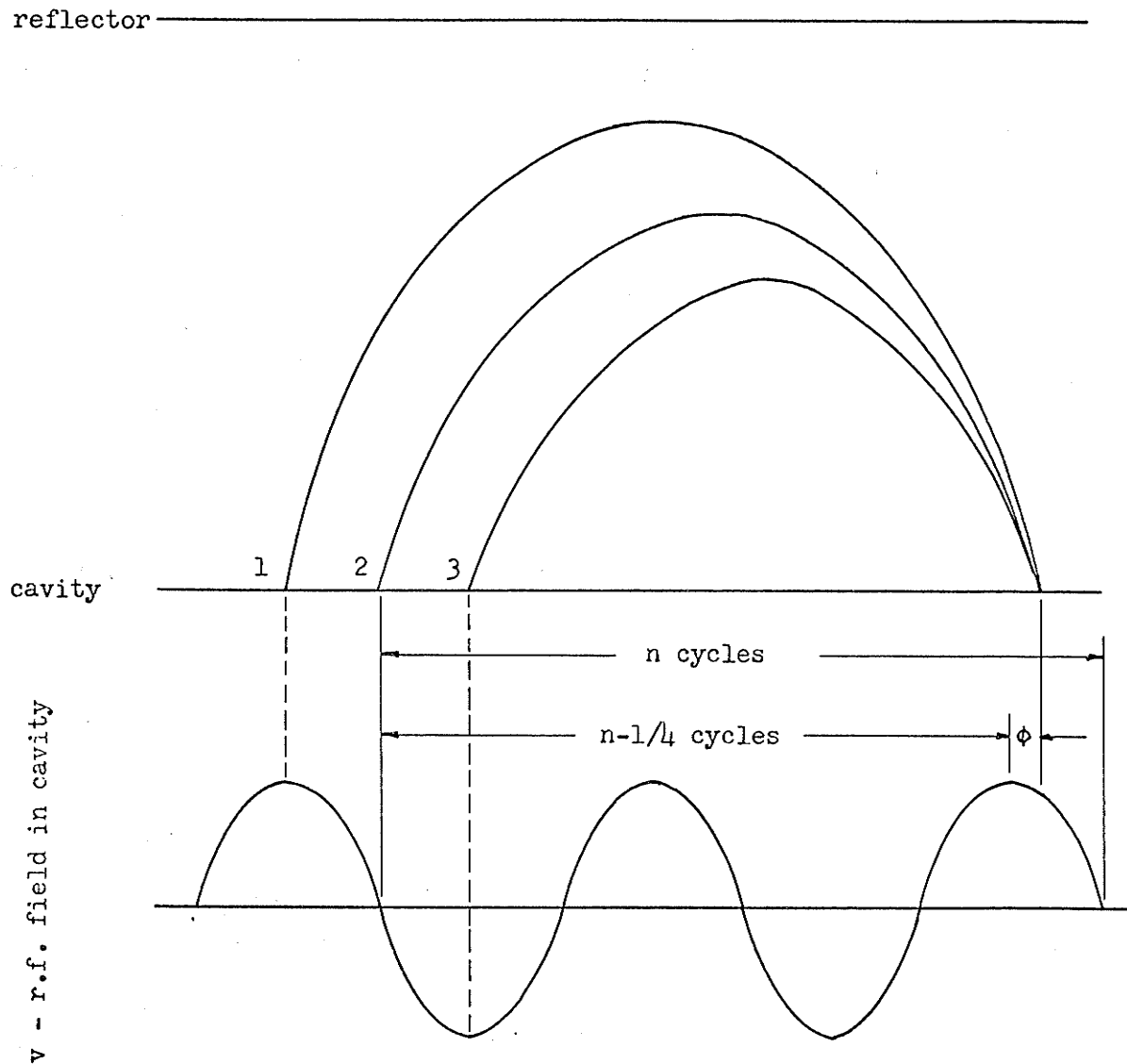


Figure 5: Time-position diagram showing the bunching process of a reflex klystron

Figure 5 shows a position-time diagram for electrons in the time interval from leaving the cavity to reentering it. The vertical

axis, between cavity and reflector, is the position of the electron in the drift space. The horizontal axis shows time. Below this, the r.f. field in the cavity is graphed as a function of time. As stated above, the reflector potential is negative with respect to the cavity, thus reversing the direction of motion of the electrons, as shown in Figure 5. Electron number one undergoes maximum acceleration in the cavity and thus leaves the cavity with a greater velocity than electrons two or three. Electron two leaves the cavity at the same velocity that it had on entering the cavity. Electron three is decelerated. Thus, if the reflector potential is the right value, bunches will form.

As can be readily seen from Figure 5, bunches form around electrons leaving the cavity when the field is zero and changing from accelerating to decelerating. Maximum energy is given up to the field when a bunch enters the cavity at a time when the r.f. field is maximum retarding. This means that the optimum transit time for an electron bunch is

$$N = n - 1/4 \text{ cycles} \dots\dots\dots 3.1$$

However, a klystron will oscillate for a transit time different from the above value, although the oscillations have a smaller amplitude. From Figure 5, it is obvious that oscillations will not occur for

$$1/4 \leq \phi \leq 3/4 \dots\dots\dots 3.2$$

where ϕ is the beam phase angle.

Since transit time is a function of reflector voltage, it is obvious that power output from the reflex klystron can be obtained for certain values of reflector voltage only. As stated above, maximum power output will occur at the voltage values which give a transit time of $n - 1/4$ cycles, while power output is obtained for $1/4 \leq \phi \leq 3/4$. Since the output power is a function of the energy of the cavity field at the time of reentry of a bunch, it is obvious that output power varies sinusoidally over positive half cycles of the cavity field. The regions of reflector voltage which give power output are known as the operating modes of the reflex klystron. Also, as is shown below, the frequency of the output signal varies as the tangent of the reflector voltage in our operating mode. A graphical representation of operating modes is given in Figure 6. The central mode is shown with a higher output power because bunching action is optimum for only one mode. If the reflector voltage is too high, transit time becomes too short for optimum bunching. If the reflector voltage is low, the transit time is long enough so that the mutual repulsion of the electrons will scatter the bunch.

The purpose of this discussion is to describe methods of frequency tuning of a klystron. One method is self evident. Changing the size of the cavity will change its resonant frequency. Thus the frequency of the output will change. This method is known as mechanical tuning.

Electronic tuning, that is tuning of the klystron by changing the reflector voltage, is also possible, since the beam susceptance is a function of ϕ , which in turn is obviously a function of reflector voltage⁷. Beam susceptance is the imaginary part of the beam admittance which is defined as the ratio of beam current in the cavity to r.f. voltage in the cavity. It can be shown that the normalized frequency change, f , from resonance frequency f is⁷

$$\frac{f}{f} = \frac{1}{2Q_L} \tan \phi \quad \dots\dots\dots 3.3$$

where Q_L is the loaded Q of the cavity.

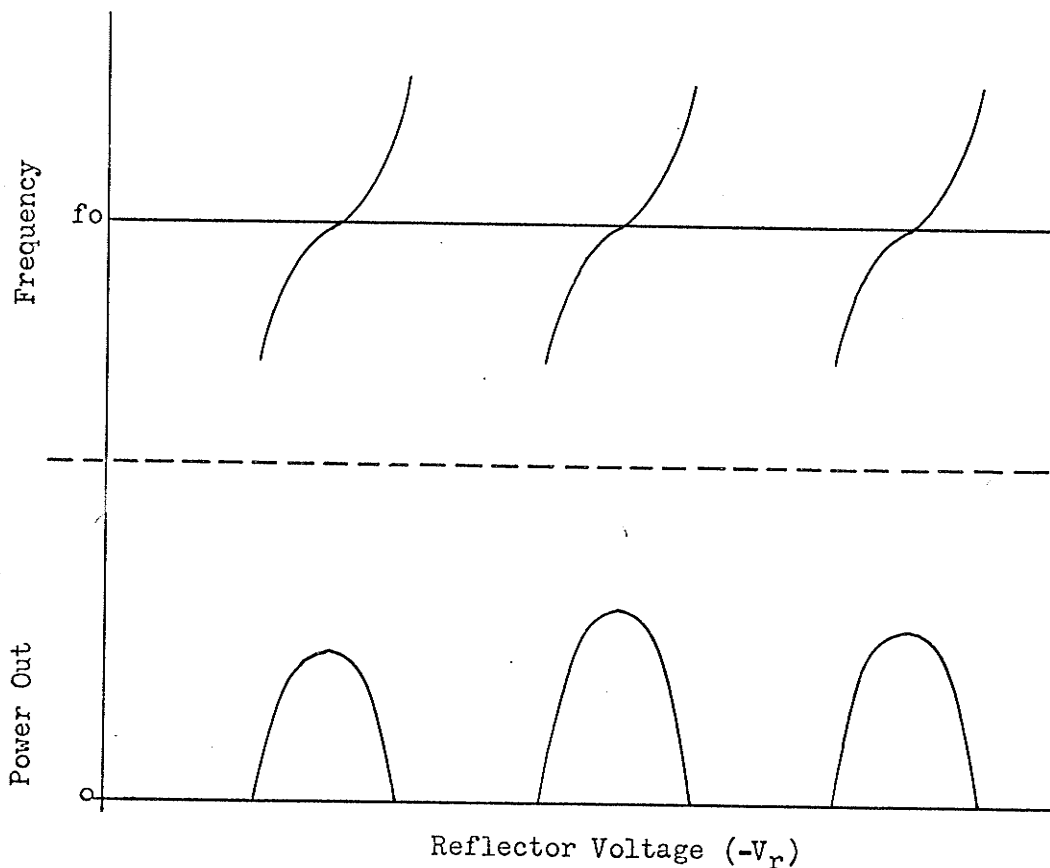


Figure 6: Operating modes of a reflex klystron

Since ϕ is a linear function of reflector voltage, $\Delta f/f$ is proportional to the tangent of the reflector voltage, within the limits of oscillations. These limits, in practice, have a much more restricted range than that given by equation 3.2. The restriction in the oscillation limits is mainly due to losses in the cavity and to loading effects. The latter can usually be suppressed by isolation of the klystron from the load. The restricted range gives a region where electronic tuning is approximately linear.

A Frequency Tracking System

As discussed in Chapter II, frequency drift due to the signal generator and local oscillator klystrons causes the main source of error in the i.f. substitution method. This problem can become so serious that measurements are impossible. The purpose of this investigation was to design and build a feedback system for the local oscillator so that it would hold the intermediate frequency, i.f., signal constant at 30 MHz. In other words, the local oscillator frequency tracks the signal generator frequency with a constant difference of 30 MHz.

Since the reflector voltage can be used to tune a reflex klystron, a d.c. error voltage proportional to frequency drift from the desired 30 MHz i.f. is applied to the reflector. If this error voltage is of the right magnitude and sign, the local oscillator changes its output frequency to compensate for the drift. To obtain the error voltage, a ratio detector, centered at 30 MHz, is used. The ratio detector has the advantage of rejecting amplitude modulation. This

means that its output voltage is proportional to frequency only and is not affected by amplitude changes of the i.f. signal. The proposed tracking system is shown in Figure 7.

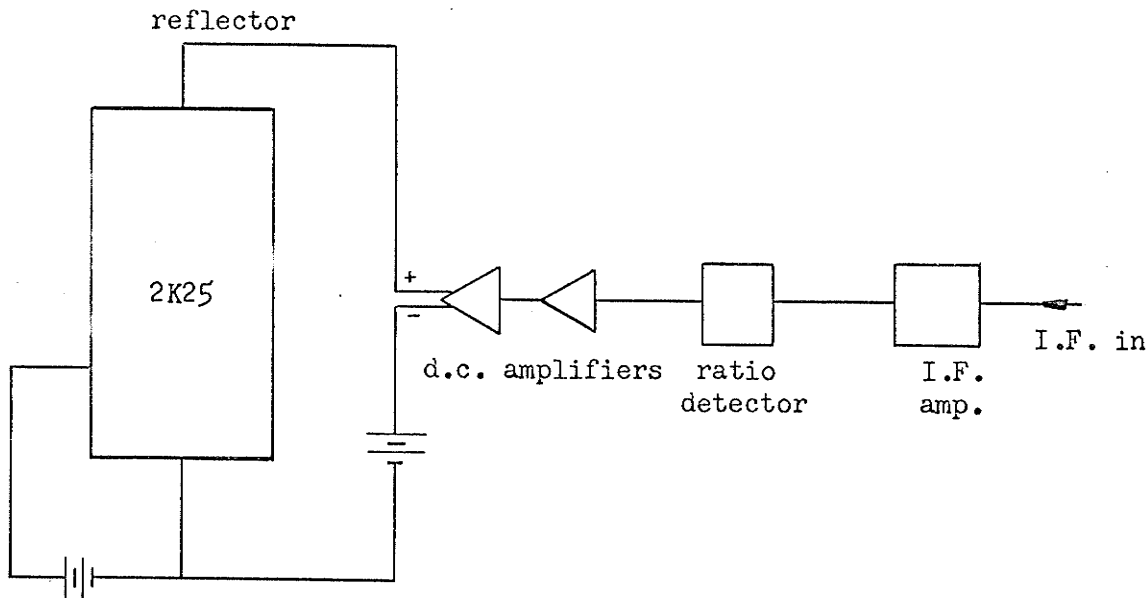


Figure 7: Frequency tracking system

The output of the mixer is fed through an i.f. amplifier and sampled by the ratio detector. The d.c. output voltage of the ratio detector is fed back to the klystron reflector through two d.c. amplifiers. These serve as buffers and have a variable gain which allows adjustment of error voltage magnitude to fit the frequency tuning curve of the klystron. Two stages are necessary to negate the inherent 180° phase shift of an operational amplifier.

CHAPTER IV

INTERMEDIATE FREQUENCY STABILIZATION

In the preceding chapter, a feedback loop to stabilize the intermediate frequency was proposed. In this chapter each block of that loop will be discussed individually. Results of tests taken on the loop as a whole are presented.

I.F. Amplifiers

Since attenuation measurements involve low signal levels, the i.f. signal must be amplified before it can be utilized as a feedback signal. Since the object was to measure high attenuations, an amplifier with large gain was designed. It was decided that a gain of about 70 db would be sufficient. Furthermore, since the linear range of a ratio detector is relatively narrow, bandwidth of the amplifier was of small concern, as long as it exceeded 1 MHz.

With these requirements in mind, a 1-stage, flat staggered-pair amplifier was designed, following the procedure outlined in reference 8. The calculations are given in Appendix A. The designed circuit is shown in Figure 8. Great care was taken in the wiring of the amplifier to make sure that it would not oscillate. It was found that shielding between the tubes was required to stop oscillations.

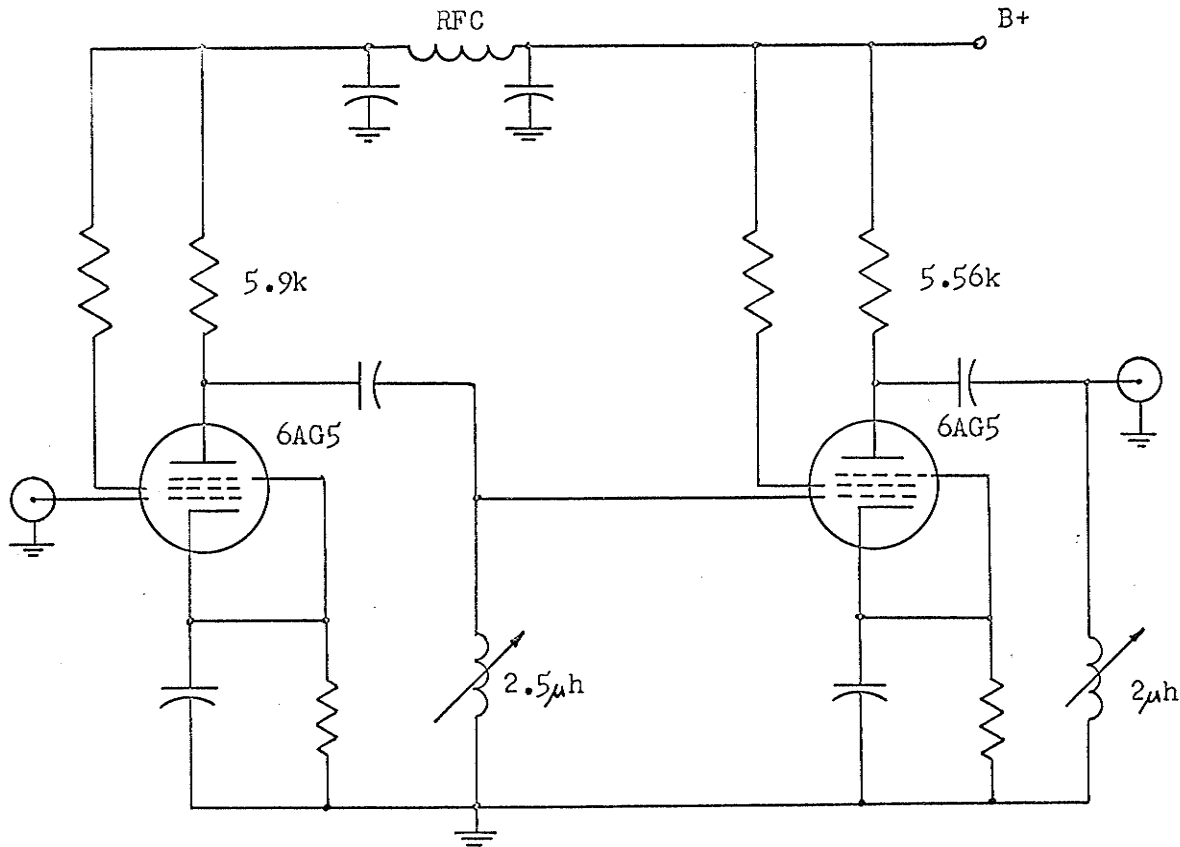
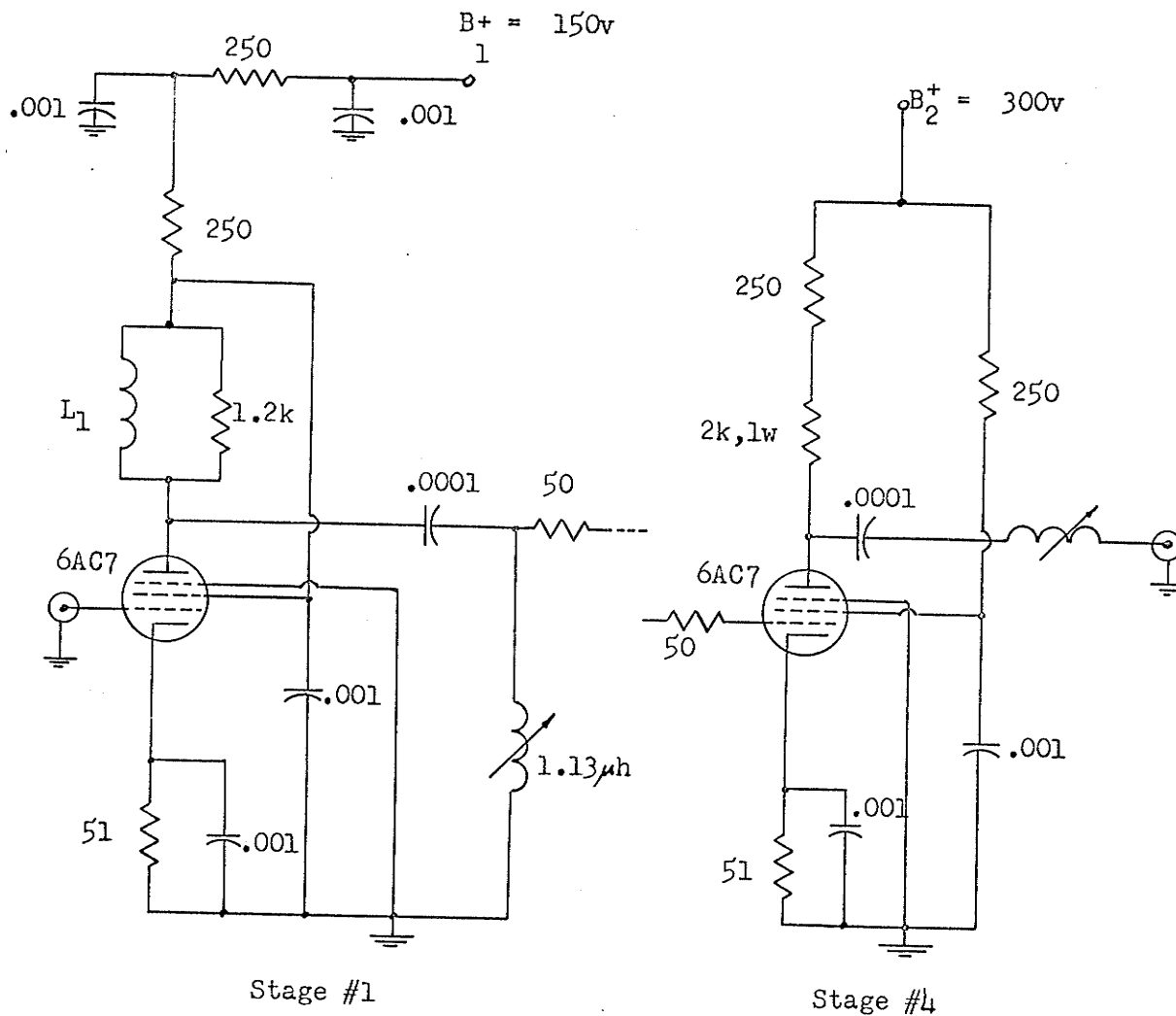


Figure 8: Flat staggered pair i.f. amplifier

According to Landee, Davis, and Albrecht³, the gain of this amplifier should have been about 55 db. However this gain could not be obtained. The gain of the amplifier was 30 db at 30 MHz with a bandwidth of 2.5 MHz. On research of the literature, it was found that a region of realizability exists for stagger tuned amplifiers⁹. The amplifier designed was outside this region. Hence the gain obtained was much lower than the expected gain.

On further search of the literature, a 6 stage, single-tuned amplifier was found¹⁰. It had a gain of 110 db at 30 MHz. A 4 stage amplifier based on this design was built as shown in Figure 9. The expected gain was 70 db.



Stages 2 and 3 same as stage 1; resistance in ohms; capacitance in μ -farads; L_1 :RFC self-resonant at 30 MHz and wound over resistor.

Figure 9: Single tuned amplifier

To stop oscillations, 50 ohm series grid resistors had to be inserted. Also, the tuning coils of the stages were put at right angles to each other and shields were inserted between stages to minimize inter-stage coupling. Furthermore, shielded leads were used in B⁺ and heater chains. After all these precautions were taken, no oscillations took place. The gain of the amplifier was found to be 50 db with a gain linearity range of 70 db, from 10 μ v to 30 mv. Its bandwidth was 2 MHz. In conjunction with an existing i.f. amplifier with a gain of 35 db, an overall gain of 85 db was obtained.

The Ratio Detector

B. D. Loughlin¹¹ was the first to develop a rigorous theory for ratio detector action in practical diodes. He developed equations and curves which can be used in designing a ratio detector. This previously had to be done empirically. Using the procedure outlined by Loughlin¹¹, the ratio detector shown in Figure 10 was designed to operate at a center frequency of 30 MHz with 30% amplitude modulation rejection. The calculations for this design are given in Appendix A.

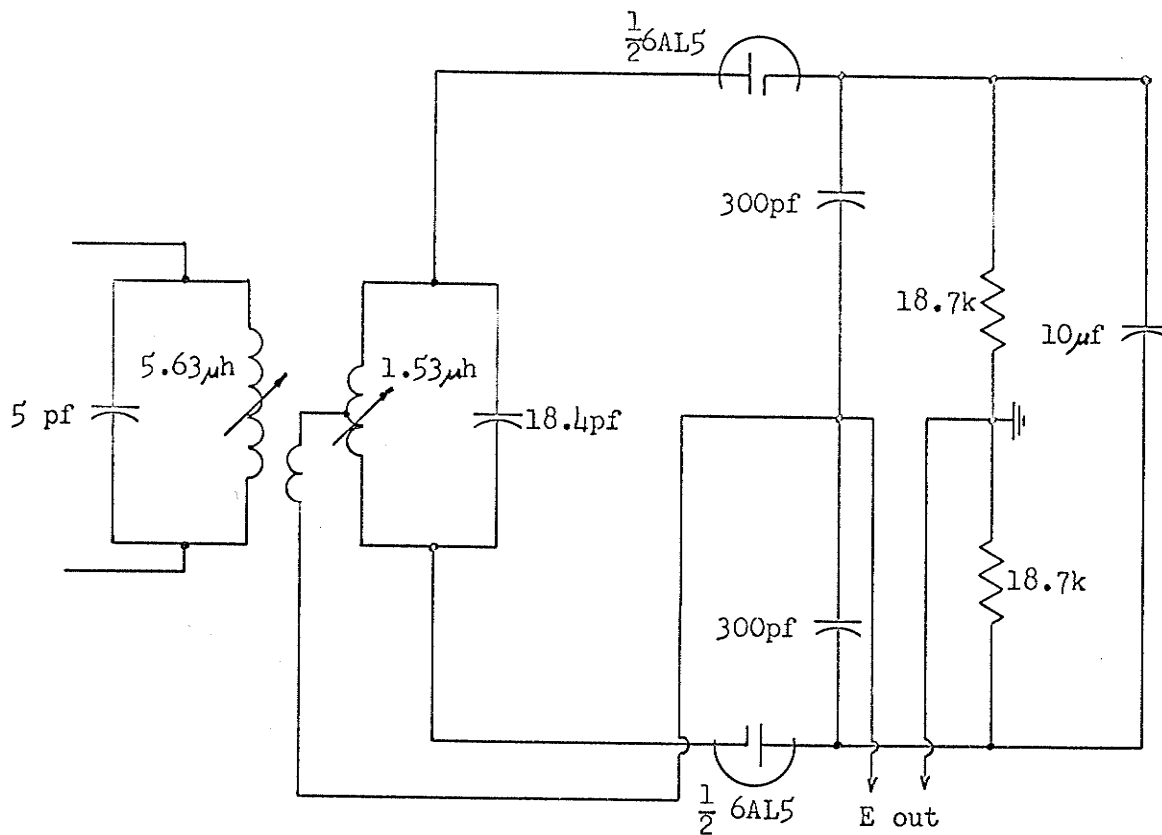


Figure 10: Ratio detector

The building and aligning of the ratio detector was done according to the suggestions given in reference 12. The tertiary was closely coupled to the primary by winding it on top of the primary. The secondary was made out of a bifilar winding. This gave an exact center tap and permitted equal tuning of both halves. To align the ratio detector, a 30 MHz signal was used at the input to the primary. The primary was tuned to give a maximum d.c. voltage at point A. Then the secondary was adjusted to give zero output voltage. Measurements were made to obtain the output characteristic of the ratio detector.

This characteristic is shown in Figure 11, which shows that good linearity was obtained. The sensitivity of the ratio detector was ± 0.084 v d.c. for a deviation of ± 100 KHz with an input voltage of 1.75 v rms.

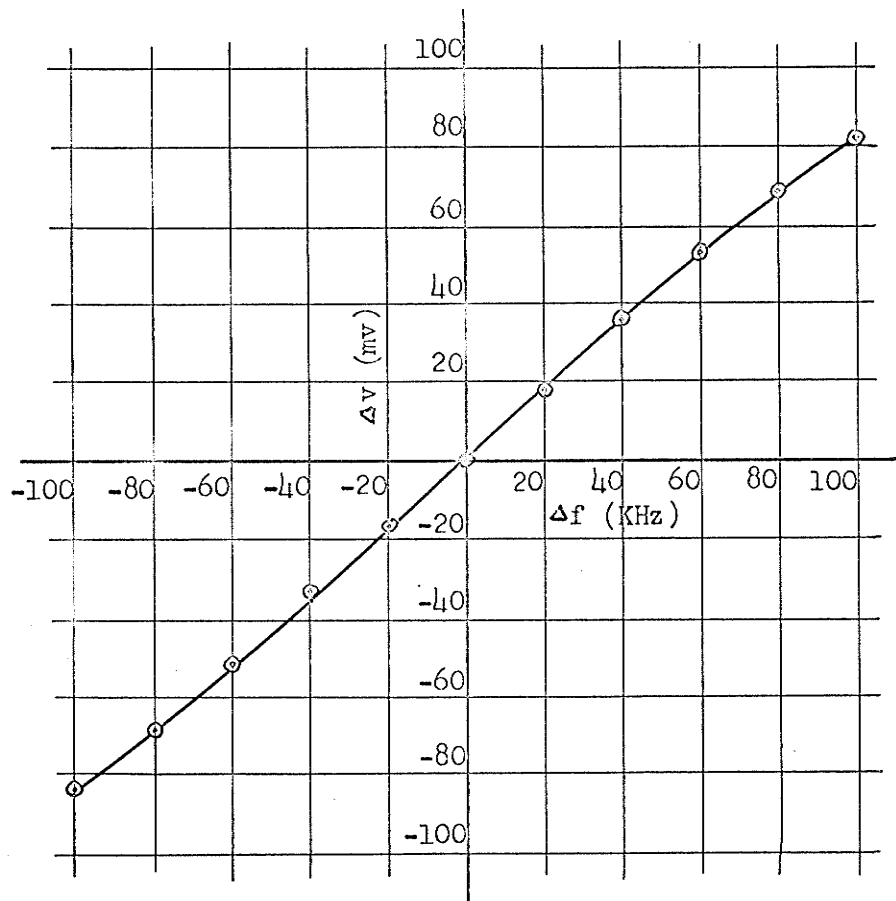


Figure 11: Ratio detector characteristic

The Stabilizing Loop

The operating characteristic of the 2K25 klystron was obtained before the loop shown in Figure 7 was assembled. The results are given

in Appendix B. Using the electronic tuning range, it was found that a reflector voltage deviation of ± 10 mv caused a frequency shift of ± 100 KHz. Since the output characteristic of the ratio detector did not fit the tuning curve for the reflex klystron, the gain of the operational amplifiers was adjusted by changing their feedback and input resistances to give a characteristic corresponding to the tuning characteristic of the reflex klystron. The feedback loop was inserted as shown in Figure 7, such that the chassis of the klystron power supply was isolated from the operational amplifier chassis.

To check system performance, the i.f. signal was displayed on a spectrum analyzer. The i.f. output contained a multitude of frequency components in a band from 20 MHz to 30 MHz. No stabilizing effect could be observed. When the loop was opened by removing the output of the operational amplifier, a single i.f. component was obtained on the spectrum analyzer. It drifted as expected and its frequency could be set by variation of either the local oscillator or the signal generator reflector voltage.

The signal components which appeared when the feedback loop was closed were most likely due to pickup of spurious signals and feedthrough from the 400 Hz stabilizing chopper of the operational amplifier. All i.f. leads were co-axial cables and the d.c. leads were made of two-wire cable with a shield. All the shields were connected to the klystron power supply chassis. However, these precautions had no visible effect on the mixer output.

Discussion of Results

No theoretical reason can be given for the failure of the loop to stabilize the i.f. signal. The problem in the loop is a technical one. All components of the system were built separately and connected as individual blocks. Since the error signal is very small in comparison with the reflector voltage, their series addition is hard to achieve. One possible solution is to integrate the feedback system and the power supply on one, well shielded chassis. The error voltage should be introduced in the regulating section of the power supply such as to affect a reflector voltage change internally instead of adding to an existing reflector voltage. Such an arrangement should overcome any technical faults existing in the original system.

CHAPTER V

ATTENUATION MEASUREMENTS

Because of the failure of the feedback loop to stabilize the i.f. signal, attempts were made to measure attenuation with the open loop system. A system was developed which minimized the time required for a measurement, hence minimizing the effect of frequency drift. These attempts are discussed in this chapter.

Measurements with the Open Loop

To investigate the feasibility of making attenuation measurements without frequency stabilization, a piece of copper screening was used as an attenuating device. The spacing of the wires was $1/16$ inch and the sample was cut large enough to cover the waveguide. It was inserted into the system by being pressed tightly between two X-band choke flanges. The device thus consisted of the screen held between the two choke flanges.

The system used is shown in Figure 12. The klystrons had been tuned individually to oscillate at approximately 30 MHz difference frequency. Their oscillating frequency was now adjusted by means of the reflector voltage to give a maximum detector current. The screen was inserted, the A.I.L. receiver attenuator set to zero, and the gain adjusted to give some convenient current reading I_1 . The

screen was removed and the attenuator setting increased to again give a current reading of I_1 . The attenuator setting is then the attenuation of the screen.

It became obvious at the outset that no usable results were obtainable with the system in this form. Readings were distributed from 20 db to 32 db. For each measurement the mechanical connections between the waveguide and the screen assembly had to be opened, the screen removed, and the two waveguide sections reconnected. This introduced an unpredictable error in the results, since mechanical connections are very difficult to duplicate. The major part of the error, however, came from the time lag due to the removal of the screen. It was felt that these sources of error caused the variable nature of the results.

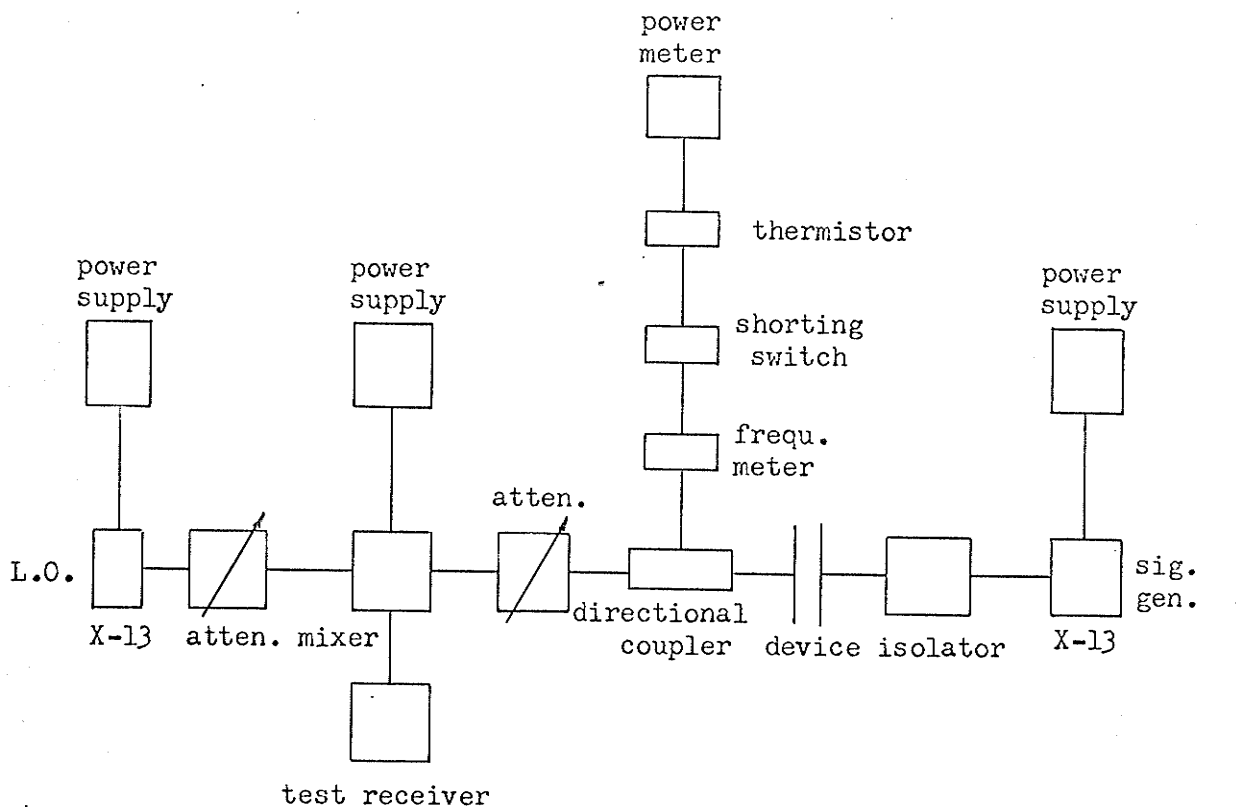


Figure 12: Open-loop system for i.f. substitution method

An Improved System

The system shown in detail in Figure 13 was developed to minimize effects of time lag and to eliminate errors caused by the non-repeatability of connections. By means of a slotted section, the arms of the H-plane T were matched. A matched condition was obtained by tuning of the slide screw and the E-H tuner such that maximum power was read on the power meter. A check was made on this by putting a slotted section in each of the arms of the H-plane T. The voltage standing wave ratio, VSWR, was measured when the above condition was satisfied and was found to be less than 1.01. The isolator and attenuator were introduced to minimize reflections from the arm not in use. The klystron power supplies were fed from a Sola constant voltage transformer which also helped to cut down the fluctuations of the detected output.

Measurements proceeded as follows. Initially the klystrons were tuned mechanically and electronically such that they were operating at the center of a mode when they were at a 30 MHz difference frequency. This tuning gave two advantages, amplitude stability as well as minimum frequency drift with repeller voltage changes. The screen was inserted in arm two and the precision attenuator in arm one was set to 20 db to reduce the power level to a value which was in the linear range of the mixer, i.e. less than -10 dbm. The slide screw tuner and the E-H tuner were adjusted to give a maximum power reading, in other words the lines were matched. With the signal feeding

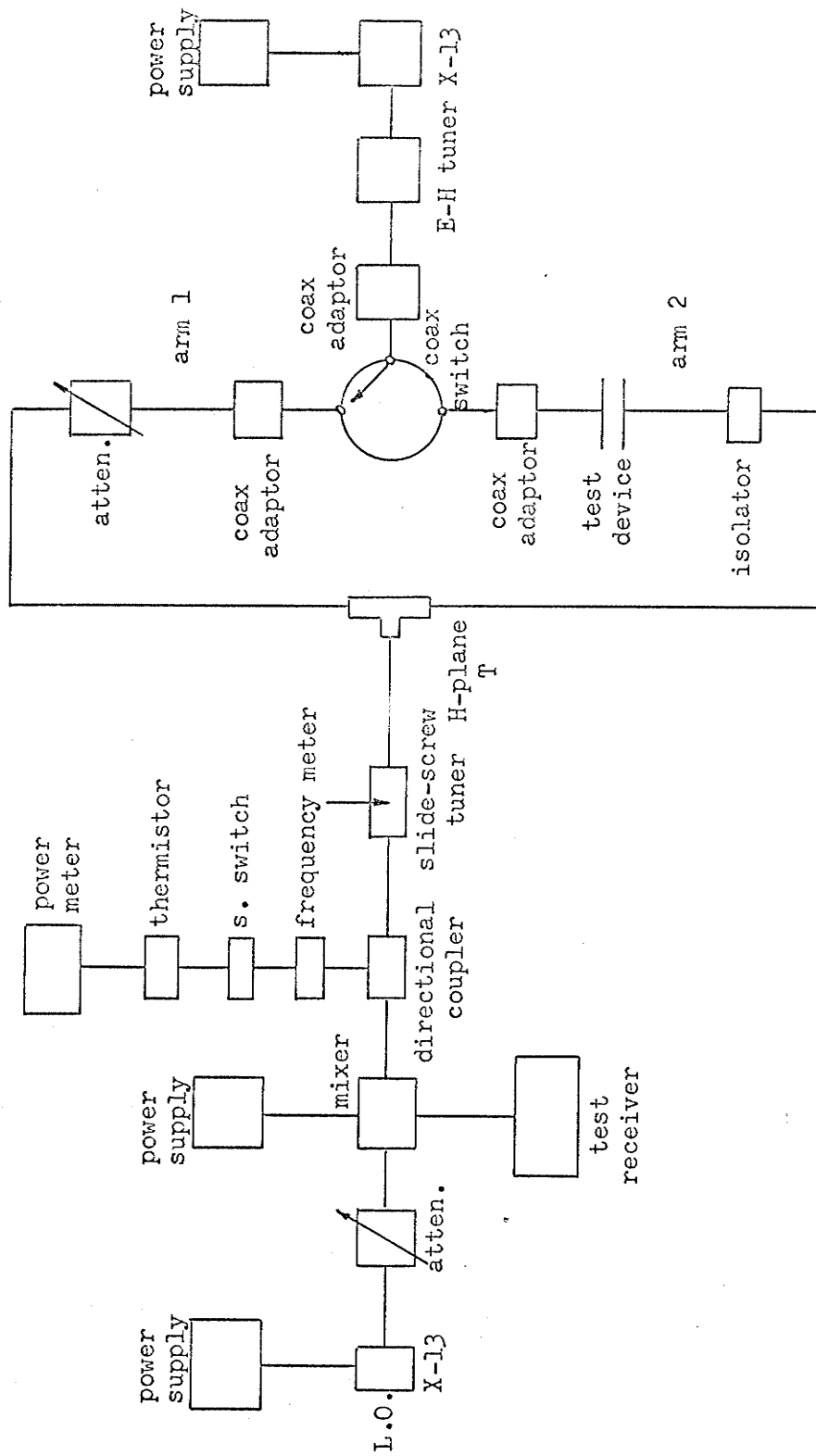


Figure 13: Improved system for the i.f. substitution method

through arm two, the input attenuator on the receiver was set to zero, and the gain adjusted to give a convenient detector output current reading, say I. The signal was switched to arm one and the input attenuation was increased to again give an output of I. The attenuator setting gave a comparison, in db, of the power in arm one to the power in arm two. One hundred such readings were taken to give an indication of the statistical distribution of these readings.

Since mismatches were only reduced to a VSWR of 1.01 and the isolator introduced insertion loss, the transmission difference of the two arms was obtained. The screen was removed from arm two. The above procedure was then used, except that the order of readings was reversed, that is the signal strength in arm one was obtained first, then the 30 MHz attenuator was set to give the same reading from arm two. Again one hundred readings were taken. The sum of the averages of the results from the two above steps gave the attenuation of the screen.

CHAPTER VI

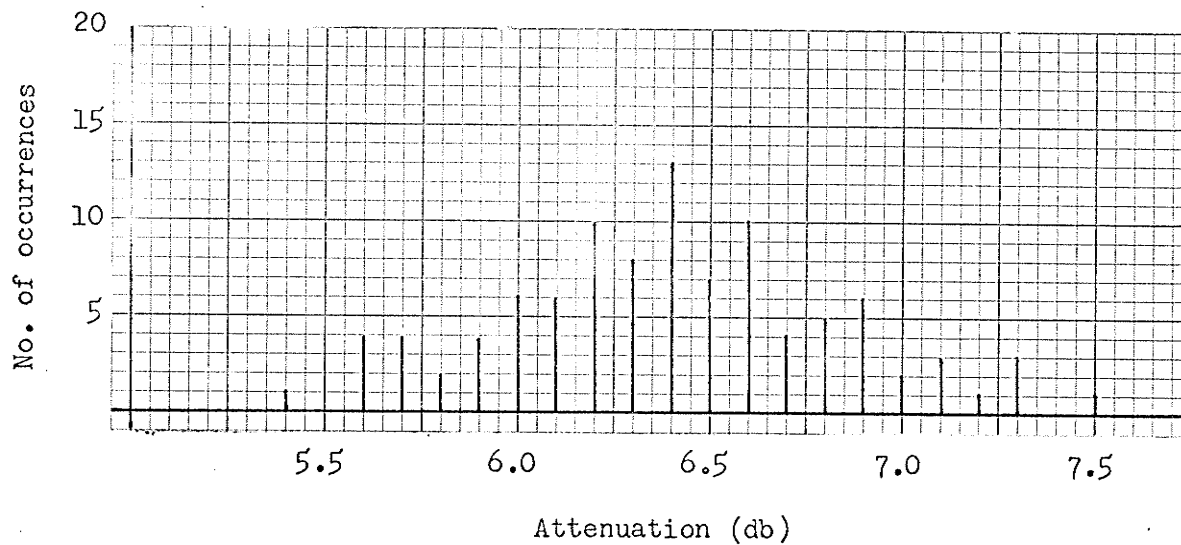
INTERPRETATION OF RESULTS

As discussed in Chapter II, the two most important criteria to be applied to a measurement system are its dynamic range and the specification of error. The results of measurements taken are discussed and an evaluation of system performance based on these results is presented.

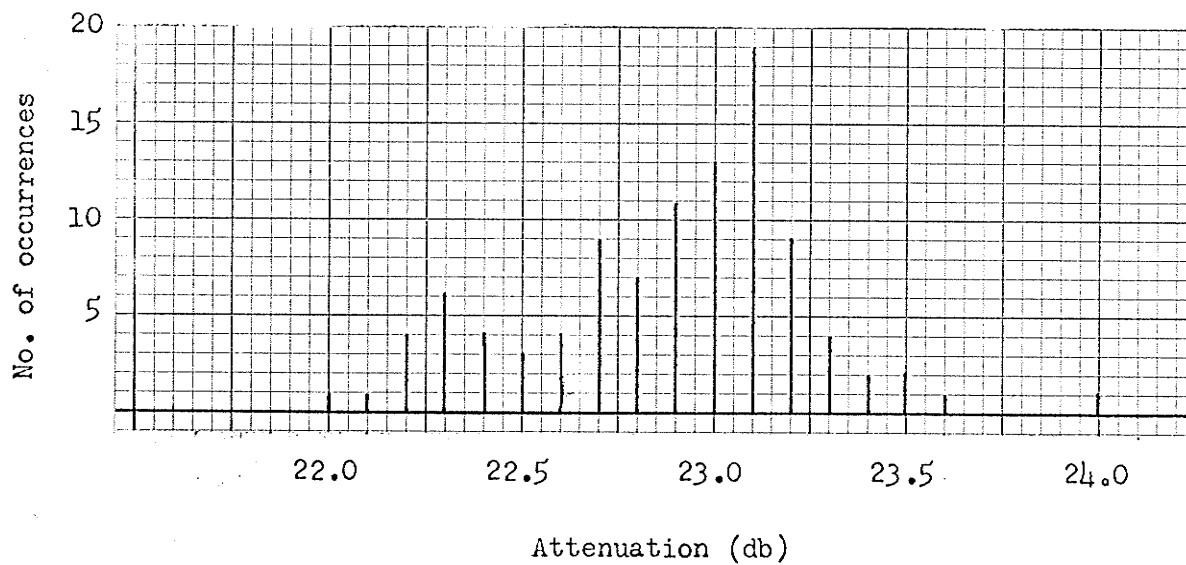
Test Results

The readings with the screen in place are shown in graphical form on Figure 14(a) and given in Table 1, Appendix C. The distribution of the readings is shown by plotting attenuations versus the number of times a particular reading was obtained. The average value of attenuator settings was 6.4 ± 0.55 db, where 0.55 db is the root mean square deviation from the mean. A similar graph, shown in Figure 14(b), was plotted for the results obtained without the screen. They are given in tabular form in Table 2, Appendix C. The average value of these results was 22.9 ± 0.36 db, where 0.36 db is again the root mean square deviation.

The run of the above two results yields the insertion loss of the screen. This value was 29.3 ± 0.91 db. The deviation of 0.91 db represents an error of about 3%. Most of this error is due to the random nature of the frequency drift. Other sources of error do exist,



14(a): Results with screen in place



14(b): Results without screen

Figure 14: Distribution of Results

such as power level drift in the signal generator, drift in gain of the i.f. amplifiers, and the usual errors in meter readings. However, these do not contribute too much to the overall error.

By use of the precision attenuator, it was found that the maximum attenuation measurable in one step was 55 db. Any higher attenuation resulted in too low a signal strength, because at such low signal levels, the coaxial switch, which cannot be accurately reset, introduced errors of as much as 20 db. No such effect was observed at higher signal levels. However, the lower the level, the greater the care in setting the switch had to be. As before, the allowable maximum power input to the mixer was -10 dbm, thus giving an upper limit to the signal strength usable. If necessary, this could be extended by placing an attenuator at the input to the mixer.

To check out the upper limit on the steps measurable, the precision attenuator was set to 50 db and the attenuation determined following the procedure outlined in Chapter V. Measurement results are given in Table 3, Appendix C. The readings had a fairly wide statistical distribution. However only twenty readings were taken, since the majority of them were close to the mean of 53.9 db. The root mean square deviation was ± 4.28 db.

System Evaluation

As can be seen from the distribution of the results, this system gives meaningful results only if a large number of readings is obtained and these are averaged, since any one reading could vary as much as 1 db from the average. In other words, measurements are time

consuming and good to within $\pm 3\%$. However, the simplicity of the system in comparison to Weinschel's complex system¹ is a great advantage.

The highest attenuation measurable, 55 db, can be increased to 110 db if two steps are taken. In the first step, a 55 db attenuator is put in the arm not containing the device to be tested. The device is inserted in the other arm. The transmission difference of the two paths is now determined as described in Chapter V. The device is then removed from the system. The transmission difference is again found. The sum of the two results yields the attenuation of the device. If the attenuator is accurately calibrated so that the transmission difference of the two paths without the device need not be measured, the maximum insertion loss measurable would be determined either by the linearity range of the mixer and i.f. stages or by the lowest level readable above the noise, i.e. whichever sets the least upper bound on the measurement.

The decreasing accuracy experienced as attenuation levels became smaller cannot be eliminated. However, for low insertion losses, the r.f. substitution method can be used. With accurately calibrated, variable attenuators and high power (100 mw or more) klystrons, attenuations up to 40 db can be accurately measured using the r.f. substitution method. As is shown by the results obtained, the accuracy of the i.f. method used is good from 20 db up. Thus the possibility of measuring attenuation from very low values to 110 db exists.

Discussion of Results

Because of technical problems and difficulties, the stabilizing system did not function properly. However, the components worked well individually, thus showing that the system is realizable. Although difficulties were expected with the ratio detector, none were experienced, confirming Loughlin's results¹¹.

The attenuation measuring system worked well in the range from 20 db to 55 db.attenuation in one step. However, as discussed in the preceding chapter, measurements of higher attenuations are possible if calibrated attenuators are available. It should be emphasized again that a number of measurements must be made and averaged in order to obtain a reasonably accurate result. Great care has to be taken to make all connections very tight, especially when working with low signal levels.

Conclusions

The following conclusions and suggestions, based on the results obtained, can be made:

1. Because of its simplicity, the r.f. substitution method of measuring attenuation is the better method. However, if a great dynamic range is required, the i.f. substitution method will have to be used. An i.f. system is, in comparison, very complex if good accuracy is required.

2. The feedback loop will work if the technical problem of an integrated power supply, as discussed in Chapter IV, can be solved. If an attempt at construction is made, the amplitude modulation rejection of the ratio detector should be made as large as possible and the detector peak separation should be increased. It would also be advisable to include an automatic gain control circuit in the i.f. amplifier of the feedback system.

3. The proposed i.f. system for attenuation measurements gives reasonable results. It does not require complex equipment and hence can be set up from the standard components usually available in a laboratory.

APPENDIXES

APPENDIX A
DESIGN PROCEDURES

I.F. Amplifier Design

As stated in Chapter IV, the first attempt of designing an i.f. amplifier was made using a single flat staggered-pair stage. A flat staggered-pair gives a maximally flat passband. This was the major reason for choosing this type of amplifier. As the name implies, flat staggered-pair means two stages which are stagger tuned about the desired center frequency, f_0 . This can be expressed mathematically:

$$f_1 = \frac{f_0}{\alpha}$$

$$f_2 = \alpha f_0$$

where f_1 is the resonant frequency of stage 1, f_2 is the resonant frequency of stage 2, f_0 is the center frequency of the pair, and α is the detuning factor.

Two more factors are required for design of the tuned circuits of each stage. These are δ , the dissipation factor, i.e. $1/Q$, for the pair and d , the dissipation factor for each stage.

Hence

$$\delta = \frac{\Delta f}{f_0} = 1/Q$$

where Δf is the bandwidth of the pair

$$d = \frac{\Delta f_1}{f_1} = \frac{\Delta f_2}{f_2}$$

where Δf_1 and Δf_2 are the bandwidths of stages 1 and 2, respectively.

Figure 7-20, reference 8, gives α and d as functions of δ .

In designing a flat staggered-pair, one would thus first decide on f_0 and Δf and then determine α and d .

Since $d = 1/Q$, the shunt damping resistors required for each stage are then

$$R_1 = \frac{1}{2\pi f_1 C_1 d}$$

$$R_2 = \frac{1}{2\pi f_2 C_2 d}$$

where C_1 and C_2 are the total shunt capacitances across R_1 and R_2 , respectively. C_1 and C_2 obviously include interelectrode capacitance of the tube used and wiring capacitances. All that remains to be calculated now are the inductances required to resonate the stages.

These are given by

$$L_1 = \frac{1}{(2\pi f_1)^2 C_1}$$

$$L_2 = \frac{1}{(2\pi f_2)^2 C_2}$$

Using the above equations, a flat staggered-pair was designed. First a tube with a relatively high gain-bandwidth product was selected. The 6AG5 with a GBW product of 96 MHz was selected because this type was readily available. The GBW product is given by

$$GBW = \frac{g_m}{2\pi C_t}$$

The value of 96 MHz did not account for wiring capacitance. This was assumed at 5 pf. The tube capacitances are given as 6.5 pf at the input and 1.8 pf at the output. The nominal value for g_m is 5 millimhos. Using the total capacitance, the GBW product now turns out to be 60 MHz.

Using the given tube parameters and equations and an overall bandwidth of 3 MHz, the following values were calculated.

| | | | |
|----------|----------|------------------------|--------------------|
| S | $= 0.1$ | $R_1 = 5.9 \text{ K}$ | $L_1 = 2.25 \mu h$ |
| α | $= 1.03$ | $R_2 = 5.56 \text{ K}$ | $L_2 = 2 \mu h$ |
| d | $= .07$ | | |

A bandwidth of 3 MHz was chosen to fit the bandwidth of the existing i.f. equipment. The circuit for this amplifier is shown in Figure 8.

The gain of the two stages in cascade is

$$A = \frac{(GBW)_1}{\Delta f_1} \times \frac{(GBW)_2}{\Delta f_2}$$

where the subscripts refer to the stage number. Since the stages use the same tubes, A becomes

$$A = \left(\frac{GBW}{\Delta f} \right)^2$$

Thus, the expected gain is $\left(\frac{60 \times 10^6}{3 \times 10^6} \right)^2 = 400 = 52 \text{ db.}$

Ratio Detector Design

As a first step in the design of the ratio detector, its requirements were decided. Because a 30 MHz i.f. system was to be used, the center frequency was set. The peak separation, i.e. the frequency difference between the peaks of the two tuned circuits, each of which is made up of one half of the center tapped secondary, then had to be chosen. The peak separation determines the linearity range of the ratio detector. It was decided to design for a separation of 200 KHz. The amplitude modulation rejection was chosen to be 30%. This value, it was felt, would be sufficient for the intended purpose of the ratio detector.

The design procedure, as given by Loughlin¹¹, is in part empirical and in part done by equations and nomographs derived by Loughlin. The major empirical result is the capacitance in the secondary of the input transformer. Loughlin found that a secondary capacitance of 50 pf at a center frequency of 10 MHz gave good results.



As a starting point, it was decided that the capacitor used in this case should have the same reactance at 30 MHz as the 50 pf one had at 10 MHz. This yielded a secondary capacitance, C_s , of 16.7 pf with a reactance, X_{cs} , of 320 ohms.

The amplitude modulation rejection of the ratio detector is determined by the efficiency of the diode, which in turn is determined by the load resistance, the diode conductance, and secondary conductance. To simplify calculations Loughlin plotted nomographs which determine these interrelated parameters.

The design procedure is as follows. First a high secondary Q , Q_s , is decided. A value of 100 for Q_s was picked. Using this and the ratio of peak separation to center frequency, δ_{PD} , the ratio of circuit susceptance to circuit conductance is given by

$$q = 2\delta_{PD}Q_s$$

With the value of q and the desired value of amplitude modulation rejection, M_d , the ratio of diode conductance to circuit conductance, D , and K_{OD} , a figure of merit, are determined from Figure 9(b) of reference 11. For this design problem, the following results were obtained:

$$\delta_{PD} = \frac{0.2}{30}$$

$$Q_s = 100$$

$$M_d = 30\%$$

$$q = 3.33$$

$$D = 1.2$$

$$K_{OD} = .297$$

From the equations for a parallel resonant circuit, the conductance of the secondary is given by

$$\frac{1}{g} = \frac{X_{cs}Q_s}{2} = 16 \text{ K}$$

Using Figure 9(a), the required diode efficiency, γ , is found to be 0.795. This value is required to find a second figure of merit, K_d , from Figure IV, reference 11. Then the load resistance, according to Loughlin, is given by

$$R_L = \frac{K_d}{D} \frac{1}{g}$$

K_d was found to be 1.4. Thus R_L is 18.7 K.

All that remains to be calculated are secondary inductance and primary inductance and capacitance. The primary capacitance was arbitrarily picked at 5 pf. Secondary capacitance had already been calculated at 18.7 pf, thus determining secondary inductance. Using the fact that reactances in a resonant circuit are zero, secondary inductance was calculated at $1.69 \mu\text{h}$. Since primary and secondary are both resonant at 30 MHz

$$L_p = \frac{C_s L_s}{C_p}$$

This yields a value of $5.65 \mu\text{h}$ for primary inductance.

The circuit in its completed form, including changes made during construction, is shown in Figure 10. The changes were made to give linear response. The capacitors in the output circuit were empirically determined during tests. The tube chosen was a 6AL5, which is an r.f. diode and was readily available.

APPENDIX B

REFLEX KLYSTRON CHARACTERISTICS

The measurement system used to obtain the characteristics of the 2K25 reflex klystron is shown in Figure A.1. The method used was quite simple. The reflector voltage was varied step by step through a mode and the power output and output frequency were obtained at each point. The results for the mode used in the tests described in this thesis are given in Figure A.2. To find the extremities of the electronic tuning range, an oscilloscope was hooked up as shown in Figure A.1 and the klystron reflector was modulated at 60 Hz. The same signal was used to trigger the horizontal sweep of the scope. In this way, the operating mode was displayed on the CRT screen. The frequencies at the extremities of the modes were read on the frequency meter which was set using the marker pip on the CRT display.

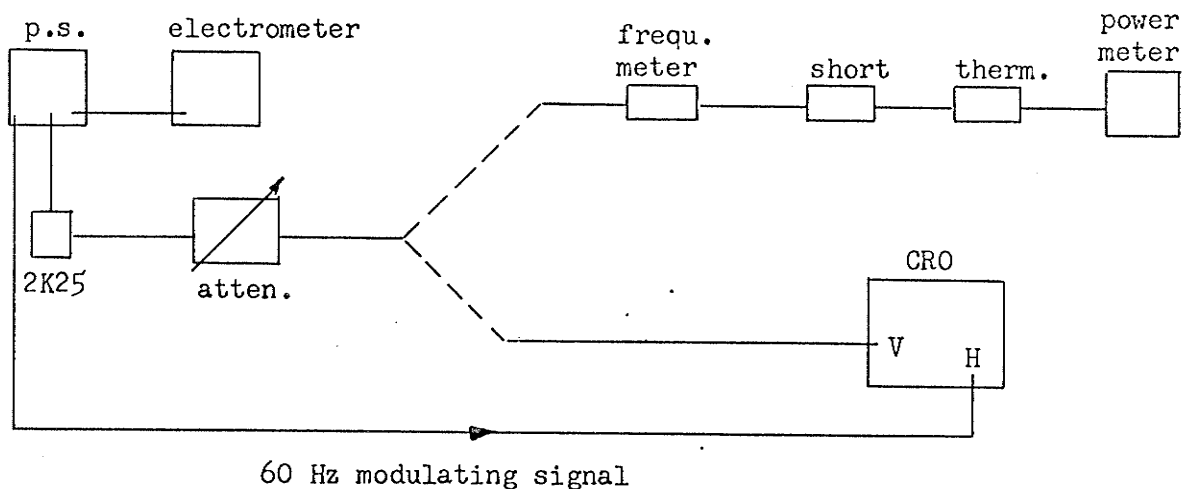


Figure A.1: Schematic for obtaining klystron characteristics

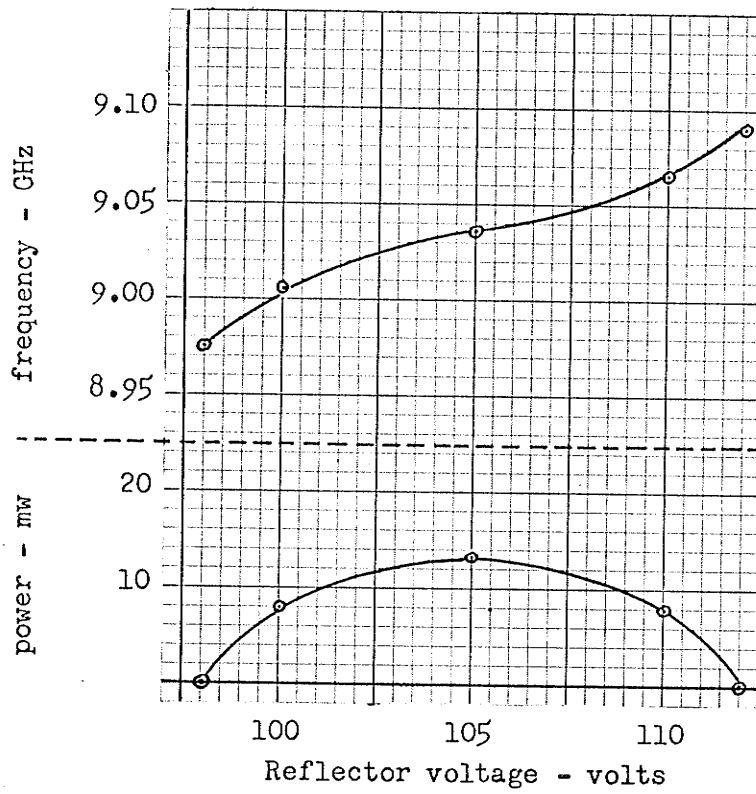


Figure A.2: 2K25 klystron characteristics

APPENDIX C

TABLES OF RESULTS

Table 1: Results with screen in place (in db)

| | | | | |
|-----|-----|-----|-----|-----|
| 6.6 | 6.5 | 6.4 | 5.6 | 6.4 |
| 6.2 | 6.6 | 6.7 | 6.6 | 6.3 |
| 5.9 | 6.8 | 6.2 | 7.2 | 6.1 |
| 6.6 | 6.6 | 6.0 | 5.7 | 6.0 |
| 6.2 | 6.4 | 6.6 | 6.5 | 6.2 |
| 6.2 | 5.6 | 7.1 | 7.0 | 6.0 |
| 6.5 | 6.0 | 5.9 | 7.3 | 6.7 |
| 5.4 | 6.7 | 7.3 | 7.1 | 6.2 |
| 6.0 | 6.8 | 6.5 | 6.1 | 6.1 |
| 5.7 | 5.9 | 6.2 | 6.5 | 6.0 |
| 6.4 | 6.4 | 6.2 | 6.4 | 6.3 |
| 6.6 | 6.6 | 5.6 | 6.2 | 6.1 |
| 5.7 | 6.6 | 6.4 | 5.5 | 5.9 |
| 6.4 | 6.6 | 6.2 | 5.8 | 7.5 |
| 6.5 | 6.9 | 6.1 | 6.3 | 7.3 |
| 6.9 | 6.4 | 6.4 | 5.7 | 6.3 |
| 6.3 | 6.3 | 5.6 | 5.8 | 6.7 |
| 6.4 | 6.8 | 7.1 | 6.3 | 6.4 |
| 6.5 | 6.9 | 6.4 | 6.9 | 6.8 |
| 6.8 | 5.8 | 7.0 | 6.3 | 6.9 |

Average = 6.4 db
RMS deviation = ± 0.55

Table 2: Results without screen (in db)

| | | | | |
|------|------|------|------|------|
| 22.8 | 23.0 | 22.0 | 22.6 | 22.9 |
| 22.2 | 22.9 | 22.4 | 23.2 | 23.1 |
| 24.0 | 22.9 | 22.2 | 23.1 | 22.9 |
| 22.9 | 22.7 | 22.3 | 23.1 | 23.2 |
| 22.8 | 22.9 | 22.2 | 23.1 | 23.0 |
| 23.1 | 22.8 | 22.3 | 23.0 | 23.3 |
| 23.1 | 22.8 | 22.2 | 22.9 | 22.9 |
| 23.5 | 23.0 | 22.1 | 22.7 | 23.0 |
| 22.3 | 22.9 | 22.6 | 22.7 | 23.2 |
| 22.4 | 22.7 | 23.6 | 23.1 | 23.4 |
| 22.4 | 22.7 | 23.2 | 23.1 | 23.0 |
| 22.9 | 22.4 | 23.2 | 23.1 | 23.2 |
| 23.0 | 22.6 | 23.5 | 23.2 | 23.0 |
| 23.1 | 22.3 | 23.3 | 23.0 | 23.0 |
| 22.9 | 22.3 | 23.1 | 23.1 | 23.0 |
| 23.1 | 22.7 | 23.0 | 23.3 | 23.2 |
| 22.6 | 22.5 | 23.1 | 23.1 | 22.5 |
| 22.7 | 22.8 | 23.4 | 23.2 | 22.7 |
| 23.1 | 22.3 | 23.1 | 22.5 | 22.8 |
| 23.1 | 22.7 | 23.0 | 23.1 | 22.8 |

Average = 22.9 db
RMS deviation = ± 0.36 db

Table 3: Results on maximum attenuation measurable (in db)

| | |
|------|------|
| 54.0 | 54.0 |
| 53.8 | 54.1 |
| 53.6 | 53.8 |
| 54.8 | 54.1 |
| 53.3 | 53.7 |
| 53.7 | 53.9 |
| 53.8 | 54.0 |
| 53.8 | 54.0 |
| 53.6 | 54.1 |
| 54.1 | 54.2 |

Average = 53.9 db

RMS deviation = \pm 0.28 db